involve
a journal of mathematics

Coexistence of stable ECM solutions in the Lang–Kobayashi system

Ericka Mochan, C. Davis Buenger and Tamas Wiandt

mathematical sciences publishers

2010 vol. 3, no. 3

INVOLVE 3:3(2010)

Coexistence of stable ECM solutions in the Lang–Kobayashi system

Ericka Mochan, C. Davis Buenger and Tamas Wiandt

(Communicated by John Baxley)

The Lang–Kobayashi system of delay differential equations describes the behavior of the complex electric field $\mathscr{E}$ and inversion N inside an external cavity semiconductor laser. This system has a family of special periodic solutions known as external cavity modes (ECMs). It is well known that these ECM solutions appear through saddle-node bifurcations, then lose stability through a Hopf bifurcation before new ECM solutions are born through a secondary saddle-node bifurcation. Employing analytical and numerical techniques, we show that for certain short external cavity lasers the loss of stability happens only after the secondary saddle-node bifurcations, which means that stable ECM solutions can coexist in these systems. We also investigate the basins of these ECM attractors.

1. Introduction

Today nonlinear delay differential equations (NDDEs) are used extensively in many fields of science and engineering. Disciplines such as population dynamics, epidemiology, financial mathematics, and optoelectronics, to name a few, use NDDEs in their modeling efforts. In most cases the model equations have very simple functional forms, yet this apparent simplicity is deceiving. They display unusually rich and complex dynamics, which primarily is a result of the high dimensionality that the time-delayed terms introduce [Hale and Verduyn Lunel 1993; Driver 1977].

Our focus is on equations modeling the behavior of external cavity semiconductor lasers. Semiconductor lasers offer many advantages not only due to their compact size but also because of their enormous application in various fields, particularly in optical data recording and optical fiber communications.

Optical feedback is inevitable in virtually all realistic applications, which can be due to, for instance, reflections from fiber facets when radiation is coupled into a fiber. From the standpoint of dynamics, an optical feedback introduces a time delay to the reinjected field which in turn makes the phase space dimension of the

MSC2000: 37G35, 37M20, 78A60.

Keywords: delay differential equations, bifurcations, Lang–Kobayashi equations.

underlying dynamical system infinite. The high dimensionality renders the analysis and understanding of external cavity lasers an extremely challenging problem from the dynamical systems point of view. As a result, our fundamental understanding about the bifurcation mechanisms leading to chaotic responses is still lacking [Davidchack et al. 2000; 2001; Erneux et al. 2000].

The performance of semiconductor lasers can be degraded significantly when the feedback is at moderate or high levels.

In general, the study of a nonlinear system often begins with an analysis of certain types of stationary solutions or fixed points. The method of study of the Lang–Kobayashi equation is similar in this respect: first we identify specific solutions, then we attempt to interpret the behavior of the model at different parameter values in terms of the location and stability properties of these specific solutions.

Lang and Kobayashi [1980] formulated a model consisting of two delay differential equations for the complex electrical field $\mathscr{E}$ and the carrier number N (see also [Alsing et al. 1996; Heil et al. 2001; 2003]). Numerical simulations have shown that these equations correctly describe the experimentally observed dominant effects. The equations are given by

$$\frac{d\mathscr{E}}{dt} = (1+i\alpha)N\mathscr{E} + \eta e^{-i\omega_0\tau}\mathscr{E}(t-\tau), \tag{1}$$

$$T\frac{dN}{dt} = P - N - (1+2N)|\mathscr{E}|^2 \tag{2}$$

where $\mathscr{E} = E_x(t) + iE_y(t)$. The physical interpretation of $\mathscr{E}$ is the complex electric field of the laser, and $N(t)$ is the carrier number density of the laser. The parameters involved are α, the line-width enhancement factor; η, the feedback strength; τ, the external cavity round-trip time; ω_0, the angular frequency; T, the ratio of carrier lifetime to photon lifetime; and P, the dimensionless pump current. The physically meaningful values we use in our investigation are $\alpha = 5,\ \tau = 5,\ T = 1710$, $P = 1.155$. These values were also used in [Heil et al. 2003]. We will make the usual assumption $\omega_0 = -\arctan\alpha/\tau$ to simplify our computations. Our bifurcation parameter will be η.

By setting $\mathscr{E} = E_x(t) + iE_y(t)$, the equations can be expressed as

$$\dot{E}_x(t) = NE_x - \alpha NE_y + \eta(\cos(\omega_0\tau)E_x(t-\tau) + \sin(\omega_o\tau)E_y(t-\tau)), \tag{3}$$

$$\dot{E}_y(t) = \alpha NE_x + NE_y + \eta(-\sin(\omega_o\tau)E_x(t-\tau) + \cos(\omega_0\tau)E_y(t-\tau)), \tag{4}$$

$$\dot{N} = \frac{1}{T}(P - N - (1+2N)(E_x^2 + E_y^2)). \tag{5}$$

We will use this form in our numerical analysis with Matlab and the Matlab package DDE-BIFTOOL [Engelborghs et al. 2002].

2. External cavity modes

Solutions to the system vary depending on the chosen values of the parameters. A certain type of solution is an external cavity mode, or ECM. The ECM is a specific solution with a constant carrier number density and constant light intensity [Rottschäfer and Krauskopf 2007]. The ECM is typically of the form

$$\mathscr{E} = E_s e^{i\phi_s t}, \quad N = N_s,$$

where E_s, ϕ_s, and N_s are constants. This can be substituted into the complex-form equations to solve for the variable ϕ_s in terms of the original parameters:

$$E_s i\phi_s e^{i\phi_s t} = (1+i\alpha)N_s E_s e^{i\phi_s t} + \eta e^{-i\omega_0\tau} E_s e^{i\phi_s(t-\tau)}, \tag{6}$$

$$0 = P - N_s - (1+2N_s)E_s^2. \tag{7}$$

Dividing (6) by $e^{i\phi_s t}$ gives us

$$E_s i\phi_s = (1+i\alpha)N_s E_s + \eta E_s e^{-i(\omega_0\tau+\phi_s\tau)}.$$

Assuming $E_s \neq 0$, the equation can be divided by E_s to find

$$i\phi_s = (1+i\alpha)N_s + \eta e^{-i(\omega_0\tau+\phi_s\tau)}. \tag{8}$$

Comparing real and imaginary parts of (7) and (8), we obtain

$$0 = N_s + \eta\cos(\tau(\omega_0+\phi_s)), \tag{9}$$

$$\phi_s = \alpha N_s - \eta\sin(\tau(\omega_0+\phi_s)), \tag{10}$$

$$0 = P - N_s - (1+2N_s)E_s^2. \tag{11}$$

To find ϕ_s, we use (9) and (10) to eliminate N_s and get

$$-\phi_s = \alpha\eta\cos(\tau(\omega_0+\phi_s)) + \eta\sin(\tau(\omega_0+\phi_s)).$$

Then setting $\beta = \arctan\alpha$, we have

$$\tan\beta = \alpha, \qquad \sin\beta = \frac{\alpha}{\sqrt{\alpha^2+1}}, \qquad \cos\beta = \frac{1}{\sqrt{\alpha^2+1}}.$$

Using the trigonometric identity for $\sin(x+y)$ we obtain

$$-\phi_s = \eta\sqrt{\alpha^2+1}\,\sin(\arctan\alpha + \tau(\omega_0+\phi_s)).$$

Since we are assuming $\tau\omega_0 = -\arctan\alpha$,

$$-\phi_s = \eta\sqrt{\alpha^2+1}\sin(\tau\phi_s).$$

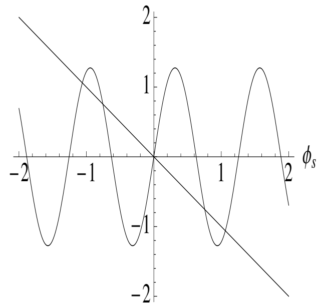

Figure 1. Graph of the two sides of (12).

The final equations are therefore

$$-\phi_s = \eta\sqrt{\alpha^2+1}\,\sin(\tau\phi_s), \tag{12}$$

$$N_s = -\eta\cos(\tau(\omega_0+\phi_s)), \tag{13}$$

$$E_s = \sqrt{\frac{P-N_s}{1+2N_s}}. \tag{14}$$

Since (12) is transcendental, a closed form solution cannot be obtained, so numerical solutions will be found. An example plot of the two sides of (12) is given in Figure 1, using our values $\alpha = 5$, $\tau = 5$, and $\eta = 0.25$. As we can see, both sides of (12) are odd functions, so for any ϕ_s solution, $-\phi_s$ is also a solution. Also, $\phi_s = 0$ is always a solution of (12), which gives us a family of equilibrium points situated on a circle in the phase-space. We will not consider the behavior of these degenerate ECMs in this paper (for different values of the bifurcation parameter η, the stability of these equilibrium points changes as well).

3. Bifurcations

ECM solutions appear as a result of saddle-node bifurcations and disappear with the occurrence of Hopf bifurcations. Changing η, the bifurcation parameter, will change the amplitude of the right side of (12). This will change the number of solutions. First, we only have $\phi_s = 0$, then by changing the amplitude, we have two new solutions at tangency points, and finally we have four solutions at four distinct intersection points. This bifurcation is demonstrated below in Figure 2. It is clear that (12) always has $\phi_s = 0$ as a solution. For the other intersections, we use the fact that at the bifurcation we have a tangency. At the point of tangency, the derivatives of both sides of (12) are equal:

$$-1 = \eta\sqrt{\alpha^2+1}\,\cos(\tau\phi_s)\tau.$$

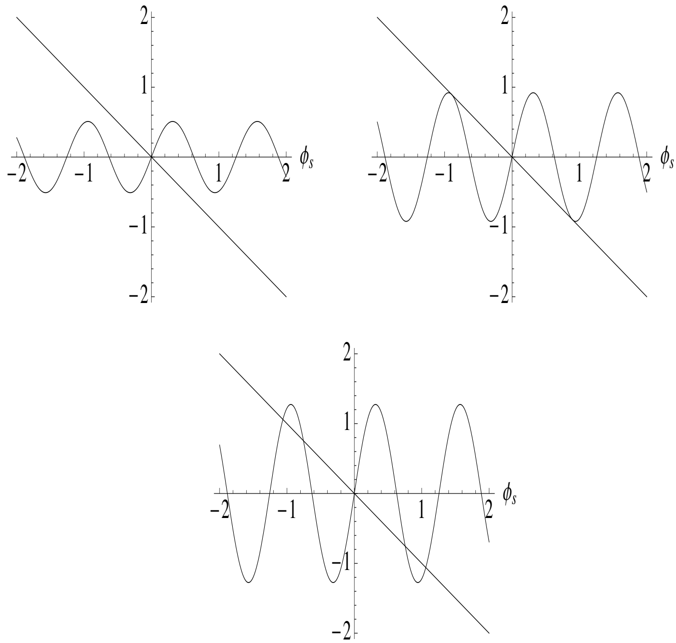

Figure 2. Example of bifurcation by changing η. Clockwise from top left: $\eta = 0.1, 0.1806, 0.25$.

So, the equations for the system at the tangency point are

$$\eta = \frac{-1}{\tau} \cdot \frac{1}{\sqrt{1+\alpha^2}} \cdot \frac{1}{\cos(\phi_s \tau)},$$

$$-\phi_s = \frac{-1}{\tau} \cdot \frac{1}{\sqrt{1+\alpha^2}} \cdot \frac{1}{\cos(\phi_s \tau)} \cdot \sqrt{1+\alpha^2} \cdot \sin(\phi_s \tau).$$

This means that at the tangency,

$$\phi_s \tau = \tan(\phi_s \tau).$$

Considering the graphs of x and $\tan x$ we can see that the solutions of the previous equation are on the intervals $((2n-1)\pi/2, (2n+1)\pi/2)$. We are only interested in the solutions on the intervals $((4n+1)\pi/2, (4n+3)\pi/2)$, because the solutions ϕ_s on the other intervals give us a negative η value. Also, asymptotically the solutions of this equation are $\phi_s \tau \sim (4n+3)\pi/2$.

For example, for our values of $\tau = 5,\ \alpha = 5,\ P = 1.155,\ T = 1710$, the first saddle-node bifurcation occurs at $\eta \approx 0.1806$, and the second saddle-node bifurcation is at $\eta \approx 0.4295$.

4. Stability of ECMs

Generally, in the case of ordinary differential equations, when a saddle-node bifurcation occurs, one of the equilibrium points created is stable and the other is unstable. In our case, the saddle-node bifurcation creates four ECM solutions (two pairs, one pair for the negative ϕ_s values and one pair for the positive ϕ_s values). In one of these pairs, both ECM solutions are unstable (when ϕ_s is positive) and in the other pair, one ECM solution is stable and the other is unstable.

As an illustration, in Figures 3 and 4 we plot two solutions for the value $\eta = 0.4$ with history $\mathscr{E} = E_s e^{i\phi_s t}$, $N = N_s$, where ϕ_s, N_s and E_s are obtained from (12), (13), and (14). The values are $\phi_s \approx -1.1382$, $N_s \approx -0.2837$, $E_s \approx 1.8250$ and $\phi_s \approx -0.6982$, $N_s \approx -0.0606$, $E_s \approx 1.760$. As the figure shows, one of the ECMs is stable and the other one is unstable.

We used the Matlab function `dde23` to create the illustration below.

The Matlab package DDE-BIFTOOL was used to analyze the stability of equilibrium points and periodic solutions. Using this package, we calculate a branch

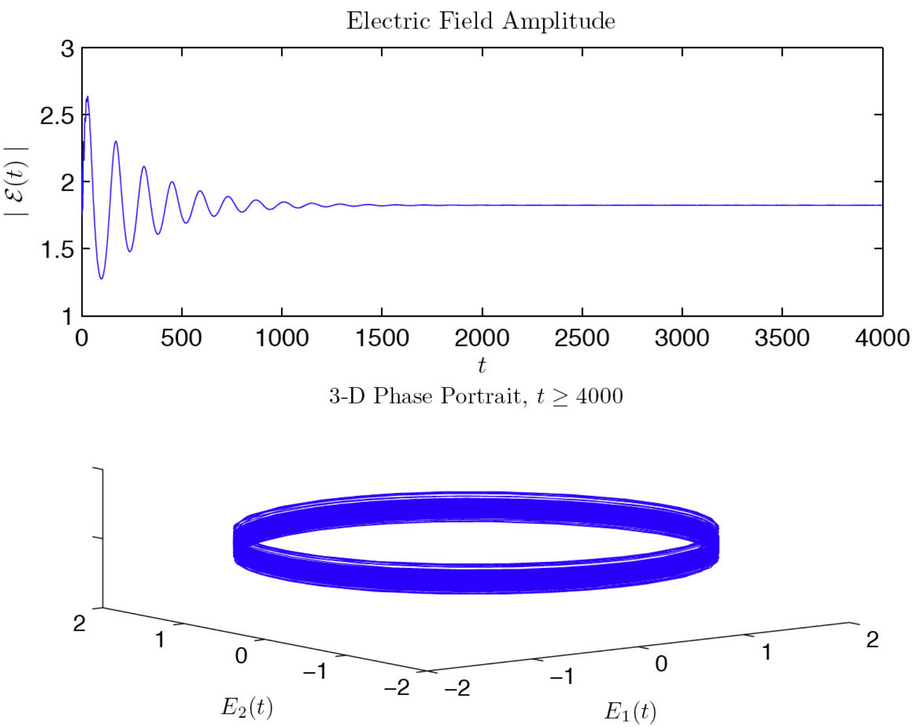

Figure 3. Stable ECM solution. The vertical coordinate in the three-dimensional graph, $N(t)$, is approximately -0.2837.

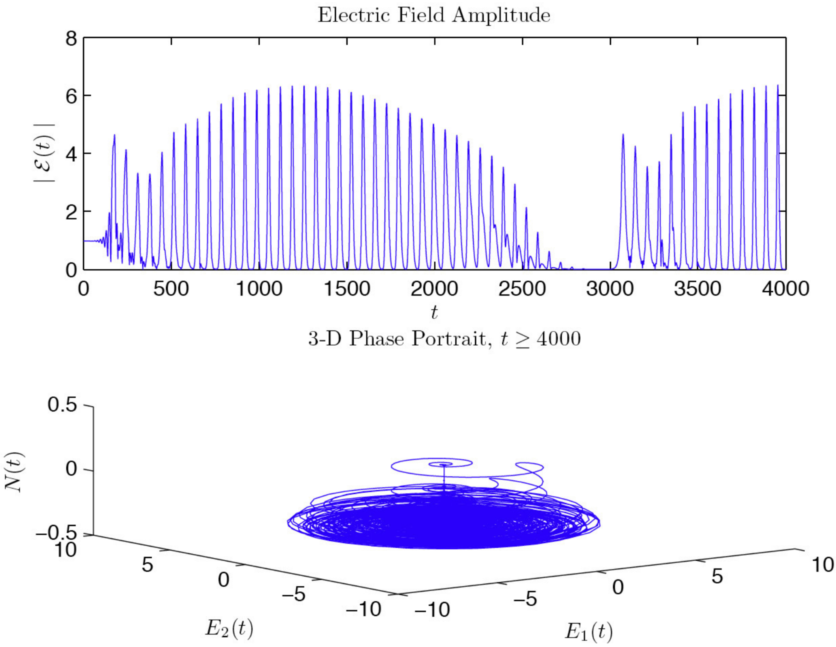

Figure 4. Unstable ECM solutions.

of ECM solutions over a range of η values. The branch plot in Figure 5 shows the amplitude of ECM solutions versus the feedback parameter η (each point on this figure represents an ECM).

On Figure 6, we show for different values of η the corresponding ECM solutions on the branch figure.

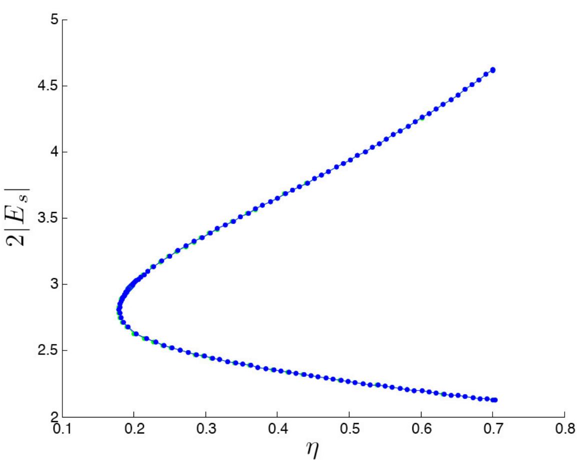

Figure 5. Branch plot from Matlab.

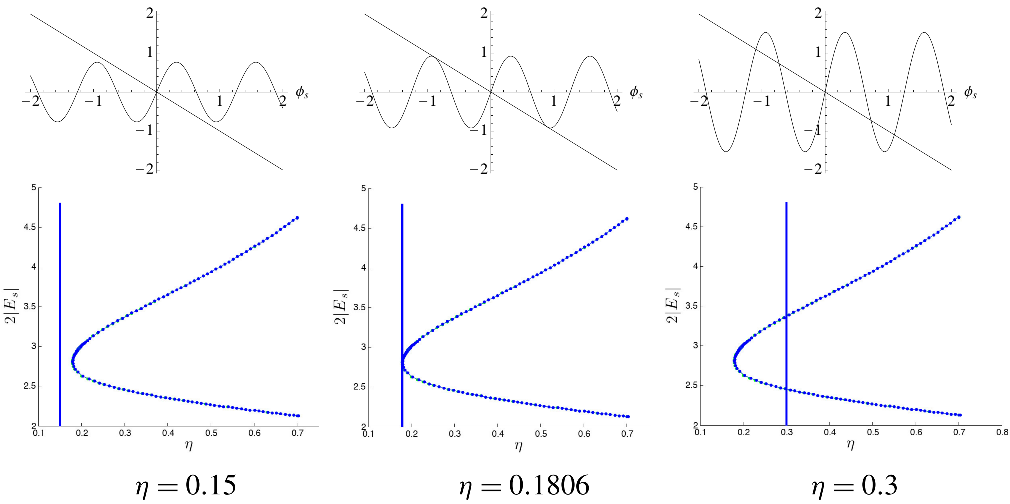

Figure 6. ECM solutions for different values of η.

Floquet multipliers are also calculated with DDE-BIFTOOL and are used to determine the stability of our ECM solutions. In order to be stable, Floquet multipliers must have an absolute value less than 1. (There is always one Floquet multiplier equal to 1, but that does not affect the stability of the periodic solution.)

The Floquet multipliers are inside the unit circle on Figure 7 (left), which proves the stability of that ECM solution. In Figure 7 (right), some of the Floquet multipliers are outside the unit circle, so the corresponding periodic solution (ECM) is unstable. This matches our numerical observations by `dde23` presented earlier in this section.

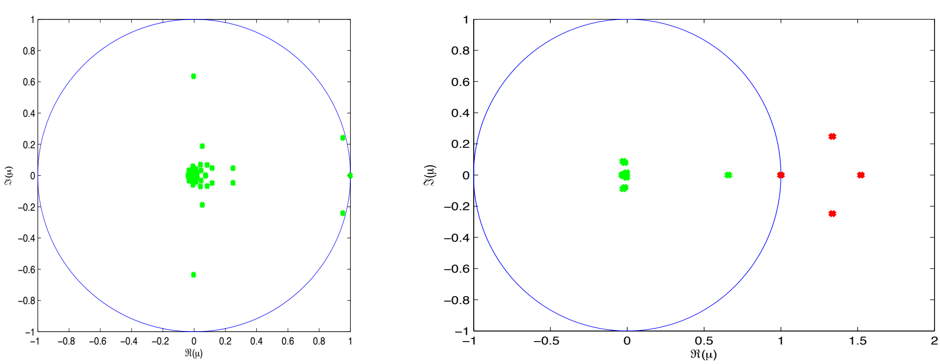

Figure 7. Floquet multipliers of stable solutions (left) and unstable ones (right).

5. Coexistence of stable ECMs and basins of attraction

Typically the leftmost ϕ_s value corresponds to the stable ECM solution and the other ECM solutions are unstable. It was observed earlier that after ECM solutions are created by saddle-node bifurcations, the stable ECM solution loses stability through a Hopf bifurcation for a slightly higher η value, and then another stable ECM will emerge through a new saddle-node bifurcation. On Figure 8, we illustrate the loss of stability through a Hopf bifurcation.

For short external cavity semiconductor lasers, there is a possibility of coexistence of two stable ECM solutions. For the $\alpha = 5$, $\tau = 5$ case, we find that the Hopf bifurcation, through which the primary ECM loses stability, occurs only after the secondary ECM is born. This creates two simultaneous stable ECM solutions. This coexistence of stable ECMs is maintained for τ values up to $\tau \approx 35$.

Using the calculated branch of the ECMs, the stability of these ECMs was determined. Figure 9 plots the absolute value of the Floquet multipliers as a function of η. Figure 9 (left) shows Floquet multipliers for the branch emerging from the primary bifurcation point, and Figure 9 (right) shows that of the branch emerging from the secondary bifurcation point. The graphs provide a rough estimate of the η value where the ECMs lose stability. Analysis of this figure reveals the coexistence of stable ECMs on the approximate range $0.43 < \eta < 0.53$.

The coexistence of two stable ECMs creates a partition in the history function space between solutions that converge to the first ECM and those that converge to the second. Of course, this function space is an infinite dimensional space, so we will consider a three dimensional subspace consisting of periodic solutions in the form $\mathscr{E}(t) = Ee^{i\phi t}$, $N(t) = N$. Figures 10–14 demonstrate the basins for the two stable ECMs for various η values. White dots indicate an initial condition function for which the solution converges to the ECM from the primary bifurcation, and

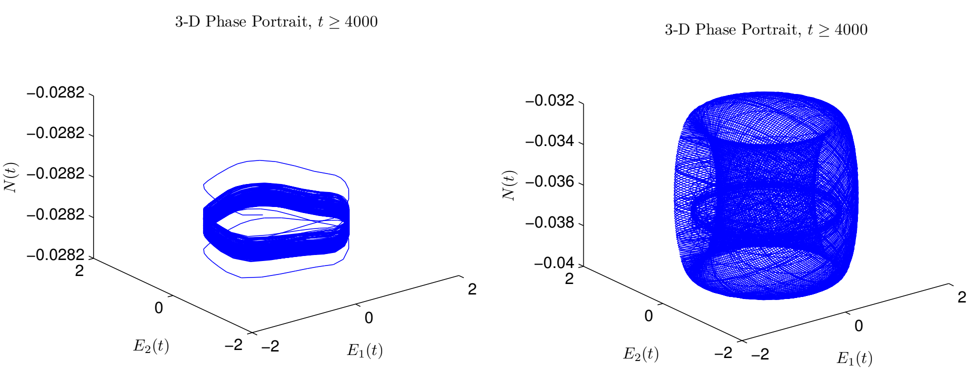

Figure 8. Left: primary ECM; right: Hopf bifurcation.

black dots indicate the initial condition functions for which the solution converges to the ECM from the secondary bifurcation. On each figure, the six subfigures correspond to the specified N value, the ϕ and E values on every subfigure correspond to the range specified on the first subfigure, divided evenly between the given values.

As these figures show, the basin of the secondary ECM attractor is growing as η increases. Accordingly, the basin of the primary ECM attractor is contracting before this ECM loses stability through the above-mentioned Hopf bifurcation at around $\eta = 0.53$.

We demonstrated that for certain short external cavity semiconductor lasers, the coexistence of stable ECM solutions is possible. Computations indicate that

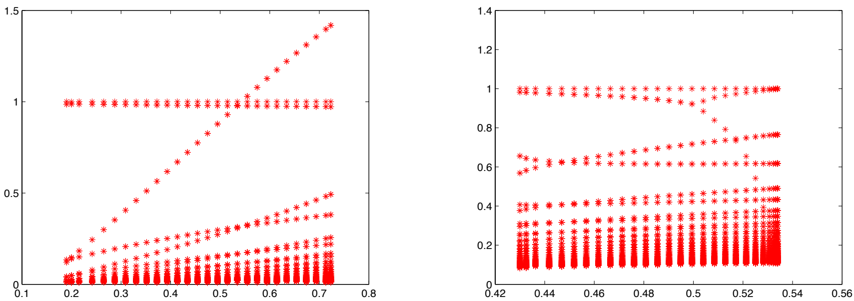

Figure 9. Floquet multipliers at the primary and secondary bifurcations.

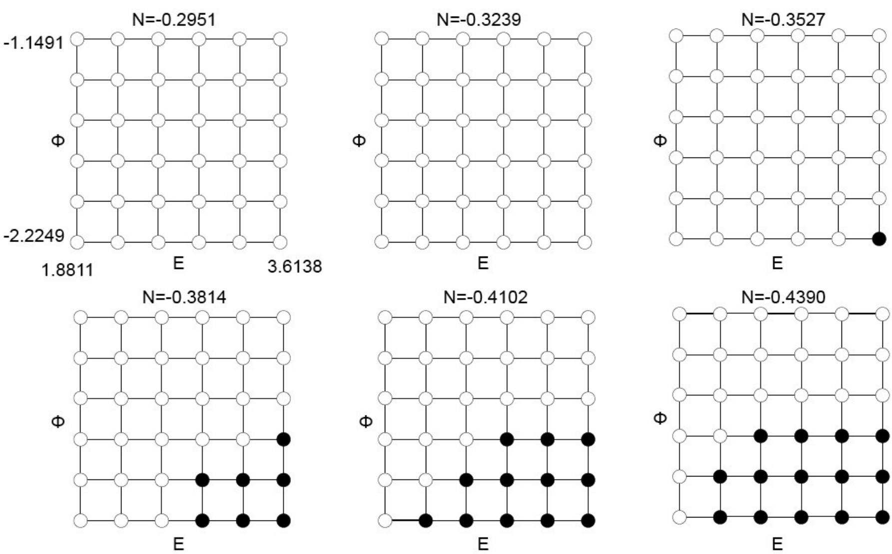

Figure 10. The case $\eta = 0.44$.

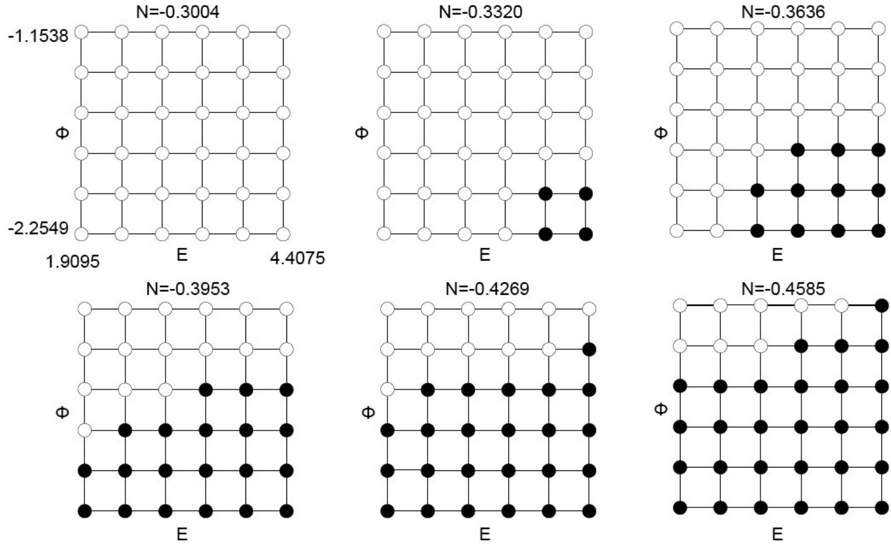

Figure 11. The case $\eta = 0.46$.

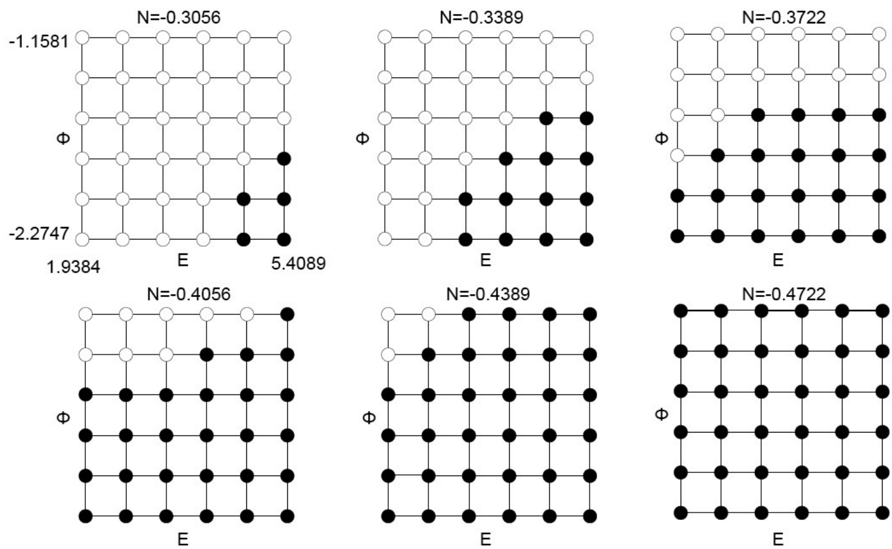

Figure 12. The case $\eta = 0.48$.

this coexistence of the stable primary and secondary ECM solutions disappear at around $\tau \approx 35$ (for the previously specified α, P, T values). This means that for short external cavities there is a range of the feedback parameter η where the laser can operate in two different modes.

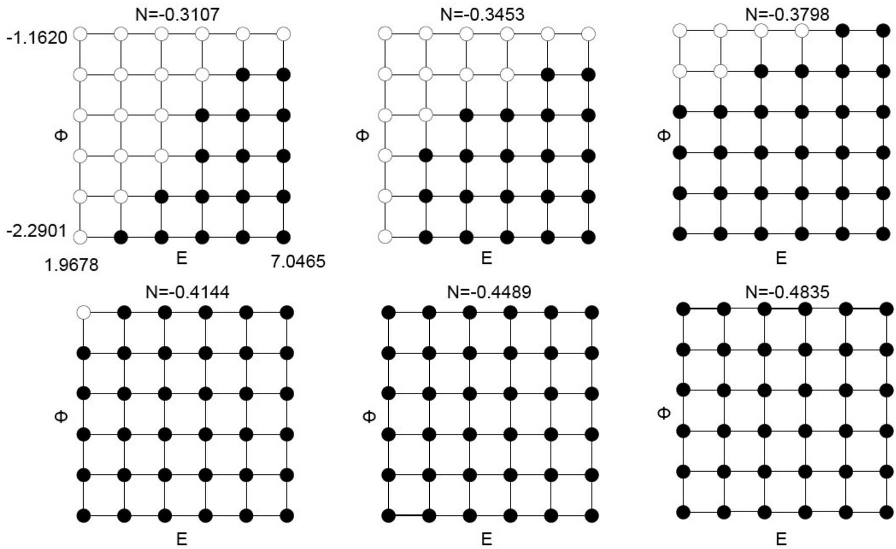

Figure 13. The case $\eta = 0.50$.

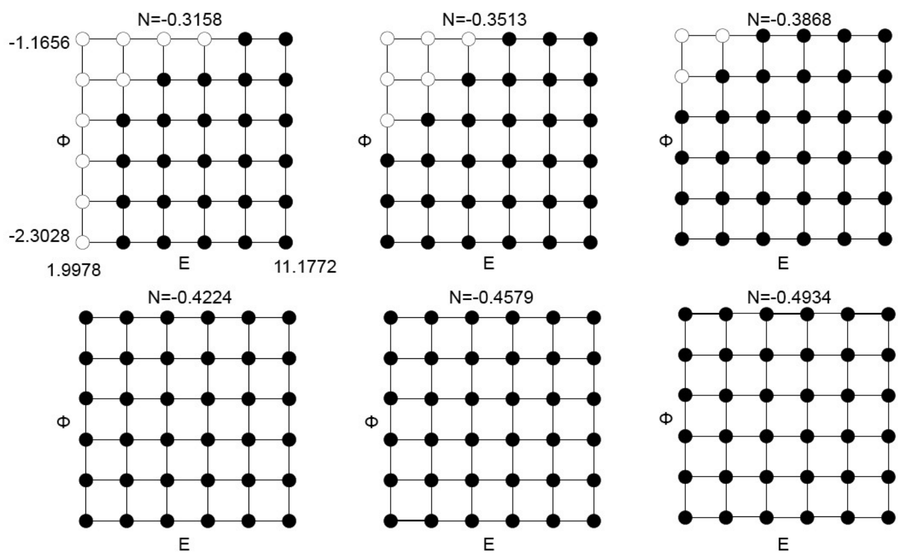

Figure 14. The case $\eta = 0.52$.

References

[Alsing et al. 1996] P. M. Alsing, V. Kovanis, A. Gavrielides, and T. Erneux, "Lang and Kobayashi phase equation", *Phys. Rev. A* **53** (1996), 4429–4434.

[Davidchack et al. 2000] R. L. Davidchack, Y. C. Lai, A. Gavrielides, and V. Kovanis, "Dynamical origins of low frequency fluctuations in external cavity semiconductor lasers", *Phys. Lett. A* **267** (2000), 350–356.

[Davidchack et al. 2001] R. L. Davidchack, Y. C. Lai, A. Gavrielides, and V. Kovanis, "Regular dynamics of low frequency fluctuations in external cavity semiconductor lasers", *Phys. Rev. E* **63** (2001), Art. 056256.

[Driver 1977] R. D. Driver, *Ordinary and delay differential equations*, Applied Math. Sciences **20**, Springer, New York, 1977. MR 57 #16897 Zbl 0374.34001

[Engelborghs et al. 2002] K. Engelborghs, T. Luzyanina, and D. Roose, "Numerical bifurcation analysis of delay differential equations using DDE-BIFTOOL", *ACM Trans. Math. Software* **28**:1 (2002), 1–21. MR 1918642 Zbl 1070.65556

[Erneux et al. 2000] T. Erneux, F. Rogister, A. Gavrielides, and V. Kovanis, "Bifurcation to mixed external cavity mode solutions for semiconductor lasers subject to optical feedback", *Optics Comm.* **183** (2000), 467–477.

[Hale and Verduyn Lunel 1993] J. K. Hale and S. M. Verduyn Lunel, *Introduction to functional-differential equations*, Applied Math. Sciences **99**, Springer, New York, 1993. MR 94m:34169 Zbl 0787.34002

[Heil et al. 2001] T. Heil, I. Fischer, W. Elsässer, and A. Gavrielides, "Dynamics of semiconductor lasers subject to delayed optical feedback: The short cavity regime", *Phys. Rev. Lett.* **87** (2001), Art. 243901.

[Heil et al. 2003] T. Heil, I. Fischer, W. Elsäßer, B. Krauskopf, A. Gavrielides, and K. Green, "Delay dynamics of semiconductor lasers with short external cavities: bifurcation scenarios and mechanisms", *Phys. Rev. E* (3) **67**:6 (2003), Art. 066214. MR 1995899

[Lang and Kobayashi 1980] R. Lang and K. Kobayashi, "External optical feedback effects on semiconductor laser properties", *IEEE J. Quantum Electron.* **16** (1980), 347–355.

[Rottschäfer and Krauskopf 2007] V. Rottschäfer and B. Krauskopf, "The ECM-backbone of the Lang–Kobayashi equations: a geometric picture", *Internat. J. Bifur. Chaos Appl. Sci. Engrg.* **17**:5 (2007), 1575–1588. MR 2008e:78022

Received: 2009-09-15 Revised: 2010-08-06 Accepted: 2010-08-19

em284475@wnec.edu *Department of Biomedical Engineering, Western New England College, Springfield, MA 01119, United States*

buenger@math.ohio-state.edu *Department of Mathematics, The Ohio State University, Columbus, OH 43201, United States*

tiwsma@rit.edu *School of Mathematical Sciences, Rochester Institute of Technology, Rochester, NY 14623, United States*

involve

pjm.math.berkeley.edu/involve

See inside back cover or http://pjm.math.berkeley.edu/involve for submission instructions.

The subscription price for 2010 is US \$100/year for the electronic version, and \$120/year (+\$20 shipping outside the US) for print and electronic. Subscriptions, requests for back issues from the last three years and changes of subscribers address should be sent to Mathematical Sciences Publishers, Department of Mathematics, University of California, Berkeley, CA 94704-3840, USA.

Involve (ISSN 1944-4184 electronic, 1944-4176 printed) at Mathematical Sciences Publishers, Department of Mathematics, University of California, Berkeley, CA 94720-3840 is published continuously online. Periodical rate postage paid at Berkeley, CA 94704, and additional mailing offices.

Involve peer review and production are managed by EditFLOW™ from Mathematical Sciences Publishers.

PUBLISHED BY

mathematical sciences publishers

http://www.mathscipub.org

A NON-PROFIT CORPORATION

Typeset in LaTeX

involve

2010 vol. 3 no. 3